

Fabrication, Characterisation and Electrochemical Properties of Heterogeneous Multiwalled Carbon Nanotubes Cation Exchange Membranes (MWCNT-CEMs)

Noor Fazliani Shoparwe, Abdul Latif Ahmad,* Nor Adibah Ahmad and
Zulfida Mohamad Hafis Mohd Shafie

School of Chemical Engineering, Engineering Campus, Universiti Sains Malaysia,
14300 Nibong Tebal, Pulau Pinang, Malaysia

*Corresponding author: chlatif@usm.my

Published online: 25 February 2018

To cite this article: Shoparwe, N. F. et al. (2018). Fabrication, characterisation and electrochemical properties of heterogeneous multiwalled carbon nanotubes cation exchange membranes (MWCNT-CEMs). *J. Phys. Sci.*, 29(Supp. 1), 41–48, <https://doi.org/10.21315/jps2018.29.s1.6>

To link to this article: <https://doi.org/10.21315/jps2018.29.s1.6>

ABSTRACT: *Heterogeneous multiwalled carbon nanotubes cation exchange membranes (MWCNT-CEMs) were successfully prepared through dry-wet phase inversion method. Different amount of MWCNTs were added into the casting solutions. The physical and chemical characteristics of the MWCNT-CEMs were analysed. The electrochemical properties of MWCNT-CEMs were examined by electrochemical impedance spectroscopy (EIS) technique. The results of impedance were fitted to the modified Randles equivalent circuit with constant phase element and restricted linear diffusion model to determine the individual parameter of the electrochemical. Modified membrane casted with 1.0 wt% of MWCNT shows the best ion-exchange capacity (IEC), the lowest membrane resistance, and the highest ion conductivity. This suggests that such amount of MWCNT provides the optimum area of conducting regions in the membrane structure to facilitate counter ions passage.*

Keywords: Cation exchange membranes, multiwalled carbon nanotubes, electrical impedance spectroscopy, MWCNT, CEM

1. INTRODUCTION

Ion exchange membranes (IEMs) are one of the most advanced separation membranes used in a large variety of applications such as electrodialysis, fuel cells, desalination and water splitting.¹ IEMs can be classified into two kinds;

anion exchange membrane (AEM) and cation exchange membrane (CEM), which depends on the added functional groups. Blending of the polymer with nanomaterial such as multiwalled carbon nanotubes (MWCNTs) have become an encouraging way to solve problems in IEMs such as low ionic flux and conductivity. The unique characteristics of MWCNTs in terms of its mechanical strength, thermal stability, electrical, and magnetic properties have made them the main choice for fabricating heterogeneous mixed matrix IEMs.^{2,3} Therefore, this research aims to fabricate the heterogeneous mixed matrix CEM by incorporating MWCNTs nanofiller. The effect of MWCNTs loading to the physical and chemical properties of the fabricated membranes were studied. Electrochemical impedance spectroscopy (EIS) method was used extensively to determine the individual resistances of CEMs system by applying alternating current (AC) across the membrane under different operating conditions. Modified Randles Equivalent Circuit with Constant Phase Element (CPE)-restricted linear diffusion was proposed and fitted with the impedance results in order to determine the important parameters such as the membrane resistance, electrical resistance, CPE, and ionic conductivity of the heterogeneous CEMs system.⁴ This study not only offers a great significant study for electrochemical properties but also on the overall performance of the heterogeneous CEMs.

2. EXPERIMENTAL

2.1 Materials

Polyvinyl-chloride (PVC) and sulfonated cation exchange resin (SCER) (Amberlyst® 15, H⁺ form) were purchased from Sigma Aldrich. N-1-Methyl-2-pyrrolidone (NMP) and acetone were supplied by Merck. MWCNT was supplied by Nano Carbons USM (20–25 nm particle size).

2.2 Preparation of CEM

Neat PVC membrane and heterogeneous MWCNT-CEMs were prepared via dry-wet phase inversion method. The composition of the casting solutions is shown in Table 1. The SCER was firstly mixed with NMP and acetone (1:1) for 3 h using magnetic stirrer. Thereafter, a calculated amount of PVC was then added into the solution and was continuously stirred overnight at 60°C to break down cluster of particles as well as to form a homogeneous solution. Each polymeric solution was casted with a casting machine (K4340 automatic Film Applicator, Elcometer) at the thickness of 300 µm. Thereafter, the membranes were exposed to air for 48 h before being immersed in distilled water at 20°C and left for 24 h to allow for solvent precipitation.

Table 1: Composition of casting solutions.

Membrane	PVC (wt%)	NMP (wt%)	Acetone (wt%)	SCER (wt%)	MWCNT (wt%)
P0	20.0	36.00	36.00	8.0	0.0
P1	20.0	35.75	35.75	8.0	0.5
P2	20.0	35.50	35.50	8.0	1.0
P3	20.0	35.40	35.40	8.0	1.5

2.3 Characterisation and Performance of CEM

Surface morphology, chemical properties and water contact angle were characterised by using Tabletop SEM (TM3000 SEM), attenuated total reflectance-Fourier transform infrared spectroscopy (ATR-FTIR, Thermoscientific Nicolet iS10) and goniometer (OCA15plus, DataPhysics), respectively. Water content of the fabricated membranes are determined by using Equation 1:⁵

$$\text{Water content (\%)} = \frac{W_{\text{wet}} - W_{\text{dry}}}{W_{\text{dry}}} \times 100 \quad (1)$$

Ion Exchange Capacity (IEC) test was carried out by using titration method.⁶ The experimental test rig for the electrochemical analysis is shown in Figure 1. Each compartment has a volume of 500 ml and the effective area of membrane used was 25.18 cm². The test cell was controlled using multi-potentiostat (VMP3, Biologic Instrument SA) with two reference electrode (RE) made up of saturated calomel electrode (SCE), and two graphite electrodes (surface area 25 cm²). The EIS experiment was carried out with the amplitude of the over imposed alternating current (AC) signal at 10 mV, and the frequency was varied between 700 kHz and 50 mHz with unequal concentrations of electrolyte at both chambers. The impedance data was simulated by using an equivalent circuit model as shown in Figure 2, where R₁ represents the membrane/electrode interfacial resistance and R₂ is the bulk resistance which was connected in series with the restricted linear diffusion impedance, Ma. CPE was connected to the circuit model because of roughness and non-homogeneity of the membrane surface. The ionic conductivity of the bulk membrane was calculated by $\sigma - 1/R_m w$, where σ is the ionic conductivity, R_m is the thickness of membrane, l is the length of the membrane, and w is the width of the membrane.

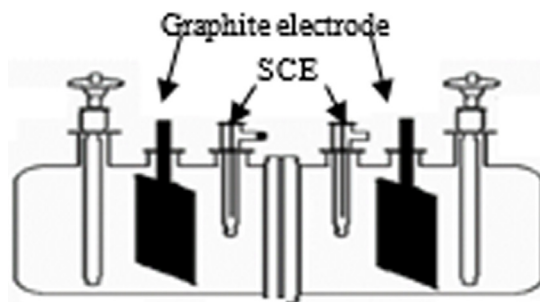


Figure 1: Schematic diagram of experimental setup.

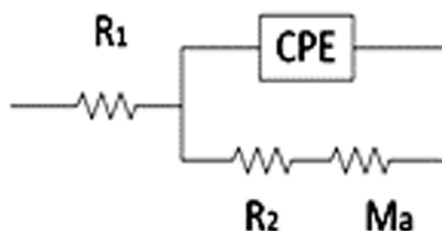


Figure 2: Equivalent circuit model.

3. RESULTS AND DISCUSSION

The SEM images of the fabricated membranes are shown in Figure 3. The obtained images confirmed that the fabricated membranes possess an open and interconnected porous structures. However, incorporation of MWCNT into the PVC matrix significantly altered the morphology of the CEMs, as shown in P1, P2 and P3. MWCNT and SCER particles were successfully embedded in the membrane matrix and caused an increase in void sizes and numbers with increasing concentrations.

FTIR spectra of neat PVC membrane and MWCNT-CEM were recorded in the range of 500–4000 cm^{-1} , as shown in Figure 4. The peaks at 2910, 1425, 1253, 1096, 959 and 680 cm^{-1} of neat PVC membrane was assigned to O-H stretching, C-H stretching, deformation C-H, C-C stretching, C-Cl stretching, and C-H wagging mode, respectively. The O-H that is originated from the polymeric matrix membrane can help to entrap water and build pathways for ion diffusion.⁷ Additional peaks were formed at 3429 and 1679 cm^{-1} after SCER and MWCNT were blended into the PVC matrix. This result shows that sulfonic acid group from SCER and MWCNT were successfully incorporated into the polymeric PVC matrix. The final thickness, water content, contact angle, and IEC of the fabricated

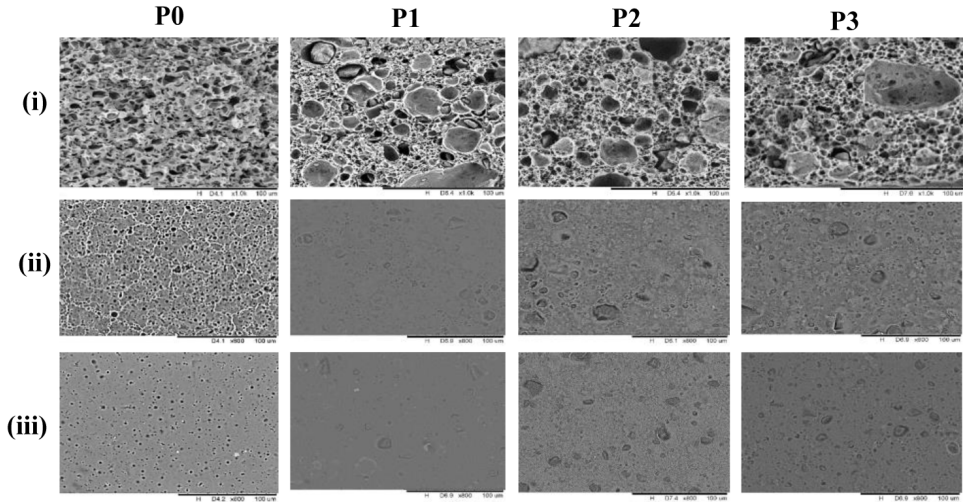


Figure 3: The SEM images of P0, P1, P2 and P3 membranes. Cross section is numbered as (i) at 1000X magnification, top surface is numbered as (ii) at 800X magnification, and bottom surface is numbered as (iii) at 800X magnification.

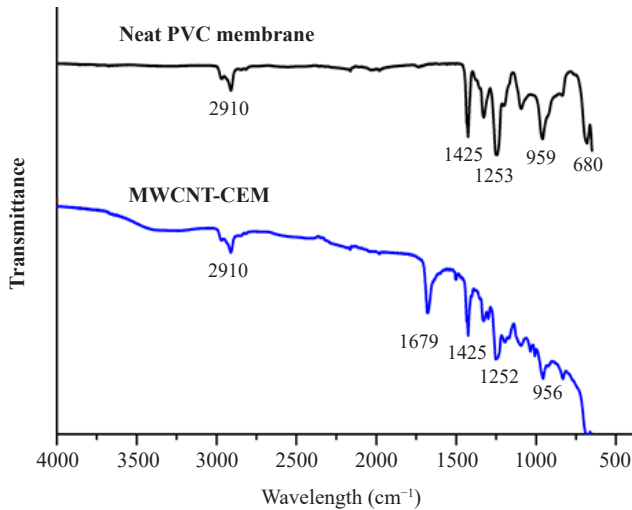


Figure 4: ATR-FTIR spectroscopy of fabricated membrane.

membranes are shown in the Table 2. The increase of MWCNT loading improves the hydrophilicity of the fabricated membrane, which influences the membrane’s capability in absorbing water. There’s also a sharp increase of water content up to P2 membrane. However, the water content decreased at higher loading of MWCNT (P3 membrane). This might be due to the increase of voids and cavities in the prepared

membranes resulting in more space for water absorption. The improvement of IEC compared to the membranes without MWCNT can be observed between P0 and P1 membrane. However, the obtained results indicated that the increase of MWCNT loading up to 1.5 wt% in the casting solution (P3 membrane) causes a decrease in IEC value. This might be due to the higher amount of MWCNT that occupied the spaces around the resin particles in the structure of the membrane. Therefore, the accessibility of ion exchange functional groups towards the spaces tends to be reduced which led to the reduction in IEC.⁸

Table 2: Final thickness, water content, contact angle and IEC of P0, P1, P2 and P3 membranes.

Sample	Thickness (μm)	Water content (%)	Contact angle ($^\circ$)	IEC (meq g^{-1})
P0	138	22.73	78.4	0.02
P1	210	42.88	55.6	0.89
P2	244	54.68	54.9	1.02
P3	251	38.41	55.2	0.82

Impedance Nyquist plot for neat PVC and MWCNT-CEM membranes are shown in Figure 5(a) and (b), respectively. The obtained Nyquist plot was similar to those found in the literature.^{9,10} The first loop of the Nyquist plot can be associated to the ionic pathway, while the second line at lower frequency (on the right) was due to the diffusion of counterions in the bulk polymeric membrane.¹¹ The Nyquist plot provides a visual verification of the good agreement between the modified equivalent circuit model and the experimental data.

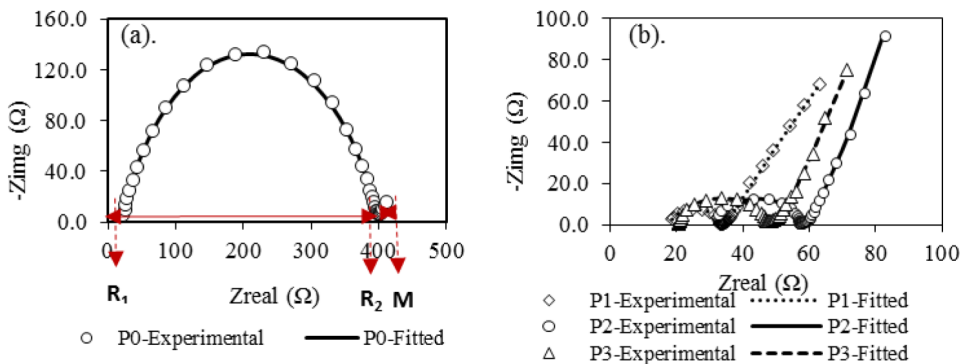


Figure 5: Experimental and generated empirical impedance Nyquist plot for (a) P0 membrane, and (b) P1, P2 and P3 membranes.

The fitted values corresponding to the data given in Figure 5 are shown in Table 3. P2 has the highest ion conductivity among the three MWCNT-CEM. As the MWCNT concentration increases, the ion conductivity also increases. However, ion conductivity decreases slightly at higher amount of MWCNT loading (above 1.0 wt%). This is likely since more compact structures were created at a higher concentration, hence the ionic exchange sites are blocked, and ion transportation paths are restricted. Besides, the ionic pathways in the membrane matrix are mostly occupied by the additive particles and thus resulting in rejection of ion transport due to the narrower channels.¹² Other researchers have also shown the improvement in CEM characteristic and performance with the addition of other nanoparticle such as Fe_3O_4 and TiO_2 into polymeric membrane matrix.^{5,8} However, the combination of SCER, PVC, MWCNT, and mixed solvent (acetone and NMP) proved to be a promising choice for CEM.

Table 3: Parameters for the impedance Nyquist plot for P0, P1, P2 and P3 membranes.

Sample (MWCNT wt%)	R1 (Ω)	CPE $\times 10^{-6}$ ($\text{F.s}^n(\text{a}0^{-1})$)	A_1	R2 (Ω)	Ma (Ω)	a0	t_1 (s)	$\delta \times 10^{-5}$ (Ω)
P0 (0%)	10.15	0.796	0.2509	375.60	2.10	0.71	0.0041	0.124
P1 (0.5%)	8.952	2.796	0.5509	23.38	8.10	0.78	0.0052	2.00
P2 (1.0%)	7.023	4.035	0.7908	23.21	10.35	0.80	0.0091	2.30
P3 (1.5%)	22.23	0.181	0.8187	36.48	9.75	0.75	0.1937	1.40

4. CONCLUSION

The addition of MWCNT plays an important role in the development of CEM as they contribute to the morphological, hydrophilicity, chemical properties, IEC, and ion conductivity changes of the membrane. MWCNT-CEM was successfully fabricated and the results indicated that water content, hydrophilicity, IEC, and ion conductivity of the membrane increased when MWCNT was increased up to 1.0 wt%.

5. ACKNOWLEDGEMENTS

The authors acknowledge the financial support provided by Universiti Sains Malaysia (USM) under the postdoctoral fellowship scheme and to Ministry of Higher Education (MOHE) Malaysia for Fundamental Research Grant Scheme (FRGS) (Grant no: 203/PJKIMIA/6071334).

6. REFERENCES

1. Strathmann, H., Grabowski, A. & Eigenberger, A. (2013). Ion-exchange membranes in the chemical process industry. *Ind. Eng. Chem. Res.*, 52(31), 10364–10379, <https://doi.org/10.1021/ie4002102>.
2. Ismail, A. et al. (2009). Transport and separation properties of carbon nanotube-mixed matrix membrane. *Sep. Purif. Technol.*, 70(1), 12–26, <https://doi.org/10.1016/j.seppur.2009.09.002>.
3. Nayak, L. et al. (2011). Thermal and electrical properties of carbon nanotubes based polysulfone nanocomposites. *Polym. Bull.*, 67(6), 1029, <https://doi.org/10.1007/s00289-011-0479-y>.
4. Bisquert, J. et al. (1998). Impedance of constant phase element (CPE)-blocked diffusion in film electrodes. *J. Electroanal. Chem.*, 452(2), 229–234, [https://doi.org/10.1016/S0022-0728\(98\)00115-6](https://doi.org/10.1016/S0022-0728(98)00115-6).
5. Hosseini, S. et al. (2014). Fabrication and electrochemical characterization of PVC based electro dialysis heterogeneous ion exchange membranes filled with Fe₃O₄ nanoparticles. *J. Ind. Eng. Chem.*, 20(4), 2510–2520, <https://doi.org/10.1016/j.jiec.2013.10.034>.
6. Hosseini, S. et al. (2012). Fabrication of (polyvinyl chloride/cellulose acetate) electro dialysis heterogeneous cation exchange membrane: Characterization and performance in desalination process. *Desalin.*, 306, 51–59, <https://doi.org/10.1016/j.desal.2012.07.028>.
7. Khoiruddin, K. & Wenten, I. G. (2016). Investigation of electrochemical and morphological properties of mixed matrix polysulfone-silica anion exchange membrane. *J. Eng. Technol. Sci.*, 48(1), 1–11, <https://doi.org/10.5614/j.eng.technol.sci.2016.48.1.1>.
8. Nemati, M. et al. (2015). Electro dialysis heterogeneous anion exchange membranes filled with TiO₂ nanoparticles: Membranes' fabrication and characterization. *J. Membr. Sci. Res.*, 1(3), 135–140.
9. Becker, C. M. et al. (2012). Sulfonation and characterization of styrene-indene copolymers for the development of proton conducting polymer membranes. *Polim.*, 22(4), 395–400, <https://doi.org/10.1590/S0104-14282012005000069>.
10. Długołęcki, P. et al. (2010). On the resistances of membrane, diffusion boundary layer and double layer in ion exchange membrane transport. *J. Membr. Sci.*, 349(1), 369–379, <https://doi.org/10.1016/j.memsci.2009.11.069>.
11. Bonastre, J. et al. (2014). Characterization of polypyrrole/phosphotungstate membranes by electrochemical impedance spectroscopy. *Synth. Met.*, 187, 37–45, <https://doi.org/10.1016/j.synthmet.2013.10.020>.